Dilated Intercavernous Sinuses: An MR Sign of Carotid-Cavernous and Carotid-Dural Fistulas

Allen D. Elster[1]
Michael Y. M. Chen[1]
Dan N. Richardson[1]
Patrick R. Yeatts[2]

Dilated venous channels traversing the sella and connecting the two cavernous sinuses were seen on contrast-enhanced MR images in four patients with angiographically proved carotid fistulas. The anatomy and variations of these so-called intercavernous sinuses are discussed and are demonstrated in Latex-injected anatomic specimens. Direct visualization of the intercavernous sinuses on contrast-enhanced MR images may serve as an ancillary sign for the diagnosis of carotid-cavernous or carotid-dural fistulas near the sella.

***AJNR* 12:641–645, July/August 1991**

Venous channels connecting the two cavernous sinuses were first described by Winslow in 1763 [1]. Since that time, the anatomy and variations of these so-called intercavernous sinuses (ICSs) have been thoroughly elucidated [2–6]. Radiologists have long been aware of ICSs, which are commonly filled during orbital venography. Additionally, ICSs are well known to angiographers as drainage pathways for carotid fistulas (CF), including those with direct carotid-cavernous connections as well as the more indirect types representing juxtasellar vascular malformations [7]. While ICSs are of continuing interest to neurosurgeons, who operate around the sella, these vessels have received relatively little attention in the recent radiologic literature, perhaps because of their small size. With the advent of high-resolution MR imaging, however, intracranial vessels of similar small size can frequently be visualized directly. We present our experience in four patients with angiographically proved CF in whom dilated ICSs were directly demonstrated on contrast-enhanced MR images.

Subjects and Methods

Four patients with clinical findings suggestive of CF were studied by CT and MR imaging. These patients, one man and three women, ranged in age from 40 to 73 years. All had presented initially with progressive proptosis and visual disturbance. In only one patient (case 1) with pulsatile exophthalmos and a loud orbital bruit was the clinical diagnosis of CF certain at presentation. In the remaining cases the diagnosis of CF was considered a reasonable clinical possibility together with other neoplastic and inflammatory diseases involving the cavernous sinuses.

Each patient first underwent high-resolution CT scanning of the parasellar region following the administration of iodinated contrast material. Axial and coronal images were obtained at 1.5-mm increments through the orbits and cavernous sinuses. All CT scans were obtained on a GE 9800 scanner (General Electric Medical Systems, Milwaukee, WI).

Next, each patient underwent high-resolution MR imaging of the sella and orbits on a 1.5-T scanner. Precontrast T1- and T2-weighted axial images were obtained using 3- to 4-mm-thick slices and other parameters appropriate for each brand of scanner. Gadopentetate dimeglumine (Magnevist, Berlex Imaging, Wayne, NJ) was administered intravenously at a dose of 0.1 mmol/kg. Multiplanar axial, coronal, and sagittal T1-weighted images were then

Received October 30, 1990; revision requested January 24, 1991; revision received February 5, 1991; accepted February 20, 1991.

[1] Department of Radiology, Bowman Gray School of Medicine, Wake Forest University, 300 S. Hawthorne Rd., Winston-Salem, NC 27103. Address reprint requests to A. D. Elster.

[2] Department of Ophthalmology, Bowman Gray School of Medicine, Wake Forest University, Winston-Salem, NC 27103.

0195-6108-91/1204-0641

TABLE 1: Clinical and Radiologic Findings in Four Patients with Carotid Fistulas

Case No.	Age	Sex	History	Physical Findings	Radiologic Findings	Final Diagnosis and Outcome
1	44	M	Severe HA and blurred vision 5 wks after head trauma	Pulsatile exophthalmos, papilledema, loud bruit	Enlarged SOV, distended anterior ICS (Fig. 1)	CF on arteriogram; treated successfully with balloon embolotherapy
2	72	F	Progressive blurred vision ×7 wks	Mild proptosis and chemosis, no bruit	SOV normal; distended inferior ICS (Fig. 2)	CF on arteriogram; spontaneous closure
3	73	F	Severe HA and progressive blurred vision ×4 mos	Mild proptosis, no bruit	Engorged sinus of dorsum sellae; enlarged SOV contralaterally (Fig. 3)	CF on arteriogram; patient being followed clinically with slight improvement
4	40	F	Severe unilateral HA and blurred vision ×6 mos	Chemosis, soft bruit developed late in course	Distended inferior ICS; SOV minimally enlarged	CF on arteriogram; treated successfully with balloon embolotherapy

Note.—HA = headache, SOV = superior ophthalmic vein, ICS = intercavernous sinus, CF = carotid fistula.

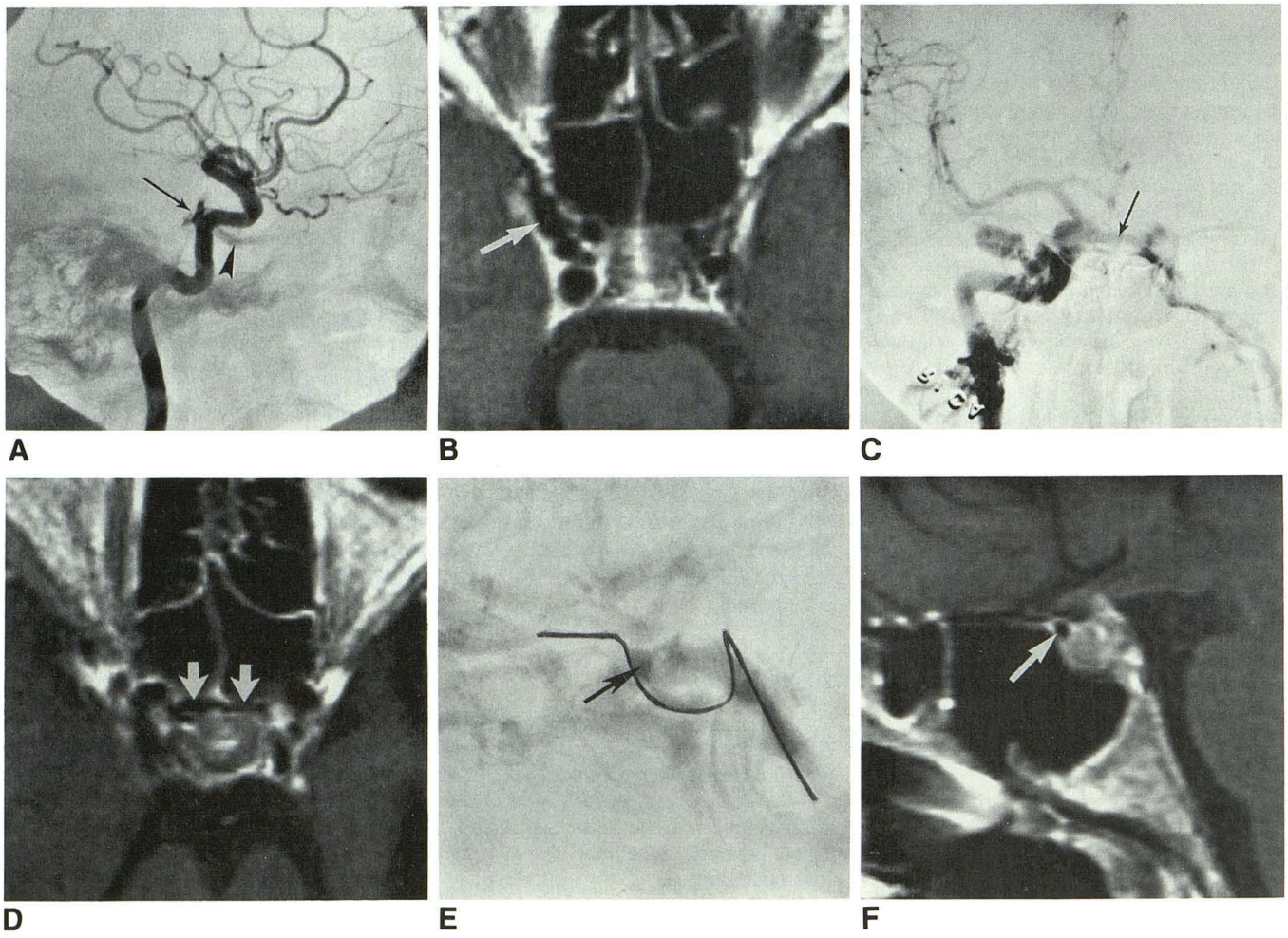

Fig. 1.—Case 1: 44-year-old man with posttraumatic carotid fistula.
***A*, Right internal carotid arteriogram, lateral view, shows dural fistula (*arrow*) with retrograde filling of superior ophthalmic vein (*arrowhead*).**
***B*, Axial contrast-enhanced T1-weighted MR image (600/20/2) shows enlarged superior ophthalmic vein at its junction with right cavernous sinus (*arrow*).**
***C*, Right internal carotid arteriogram, frontal view, shows filled transsellar venous channel (*arrow*).**
***D*, Axial contrast-enhanced T1-weighted MR image (600/20/2) shows flow void in region of anterior intercavernous sinus (*arrows*).**
***E*, Later phase of arteriogram, lateral view, shows anterior intercavernous sinus (*arrow*).**
***F*, Sagittal T1-weighted MR image (600/20/2) shows anterior intercavernous sinus to good advantage (*arrow*).**

obtained beginning immediately after completion of contrast infusion. These patients subsequently underwent selective cerebral arteriography to document the diagnosis of CF.

Following a retrospective review of the scans and arteriograms of these patients, we then carried out a direct anatomic demonstration of the intercavernous sinuses in a human cadaver. In the neck of a fresh cadaver the internal jugular veins were first exposed and tied proximally. Approximately 20 ml of blue Latex was injected into each vein with retrograde filling of the cerebral vasculature. The Latex was then allowed to harden overnight. The cadaver head was removed and solidly frozen to −10°C. Block removal of the sellar region was carried out by hand. Direct sagittal sections through the sella were obtained using a high-speed bandsaw. The specimens were inspected visually for the presence of the intercavernous sinuses.

Results

The clinical and radiologic findings in the four patients are summarized in Table 1. In only one patient (case 1) was a loud orbital bruit and pulsatile exophthalmos present to allow definitive clinical diagnosis of CF to be made at initial clinical presentation. The remaining three patients had more nonspecific clinical findings, including blurred vision, headaches, and proptosis; therefore, neoplastic and inflammatory processes were considered as possible alternative diagnoses, together with low-flow carotid-cavernous or carotid-dural fistulas. Angiographically documented CFs were subsequently identified in all four patients.

Slight enlargement or lateral convexity of the involved cavernous sinus was seen to some degree in all cases, and were seen equally well on both MR and CT. On MR, filling defects (flow voids) in the cavernous sinuses were also noted in all cases (Figs. 1B, 2B, and 3C); they were seen especially well on the postcontrast and T2-weighted MR images. Enlargement of the superior ophthalmic vein was present in three of four patients, and seen well on both MR and CT.

Engorgement of the ICS was seen in each case of proved CF. Case 1 demonstrated the anterior ICS (Fig. 1), cases 2 and 4 demonstrated the inferior ICS (Fig. 2), while case 3 showed this sinus of the dorsum sellae (Fig. 3). These vessels were not appreciated on CT, but could be discerned on precontrast MR in each case. Contrast-enhanced MR and angiography, however, demonstrated these channels to best advantage in all cases. A diagrammatic view of these intercavernous connections is presented in Figure 4.

Our single cadaveric specimen (Fig. 5) demonstrated well the anterior ICS and the sinus of the dorsum sellae. A tiny inferior ICS could also be discerned. The posterior ICS was either nondeveloped or did not fill with Latex in this specimen.

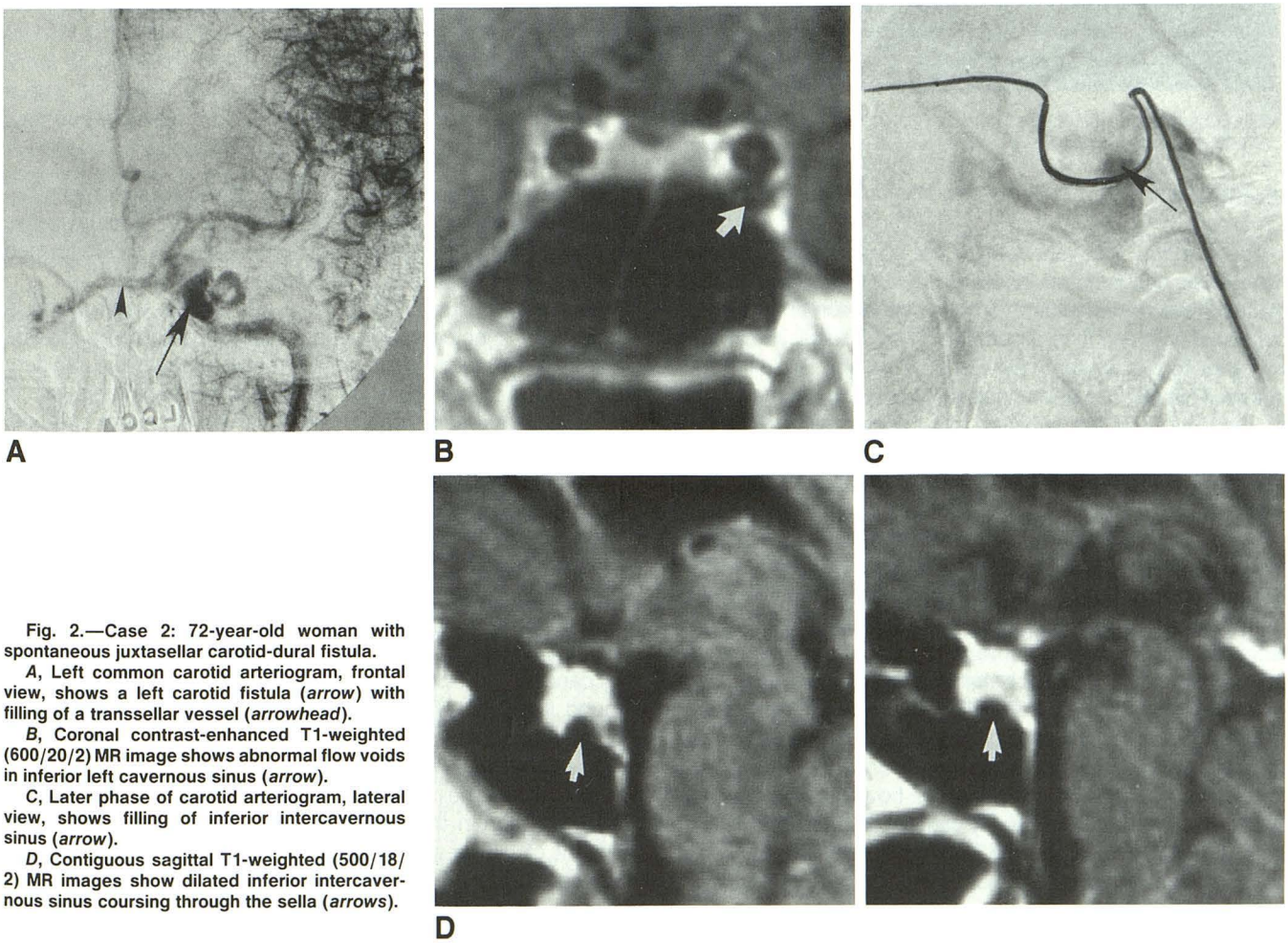

Fig. 2.—Case 2: 72-year-old woman with spontaneous juxtasellar carotid-dural fistula.

***A*, Left common carotid arteriogram, frontal view, shows a left carotid fistula (*arrow*) with filling of a transsellar vessel (*arrowhead*).**

***B*, Coronal contrast-enhanced T1-weighted (600/20/2) MR image shows abnormal flow voids in inferior left cavernous sinus (*arrow*).**

***C*, Later phase of carotid arteriogram, lateral view, shows filling of inferior intercavernous sinus (*arrow*).**

***D*, Contiguous sagittal T1-weighted (500/18/2) MR images show dilated inferior intercavernous sinus coursing through the sella (*arrows*).**

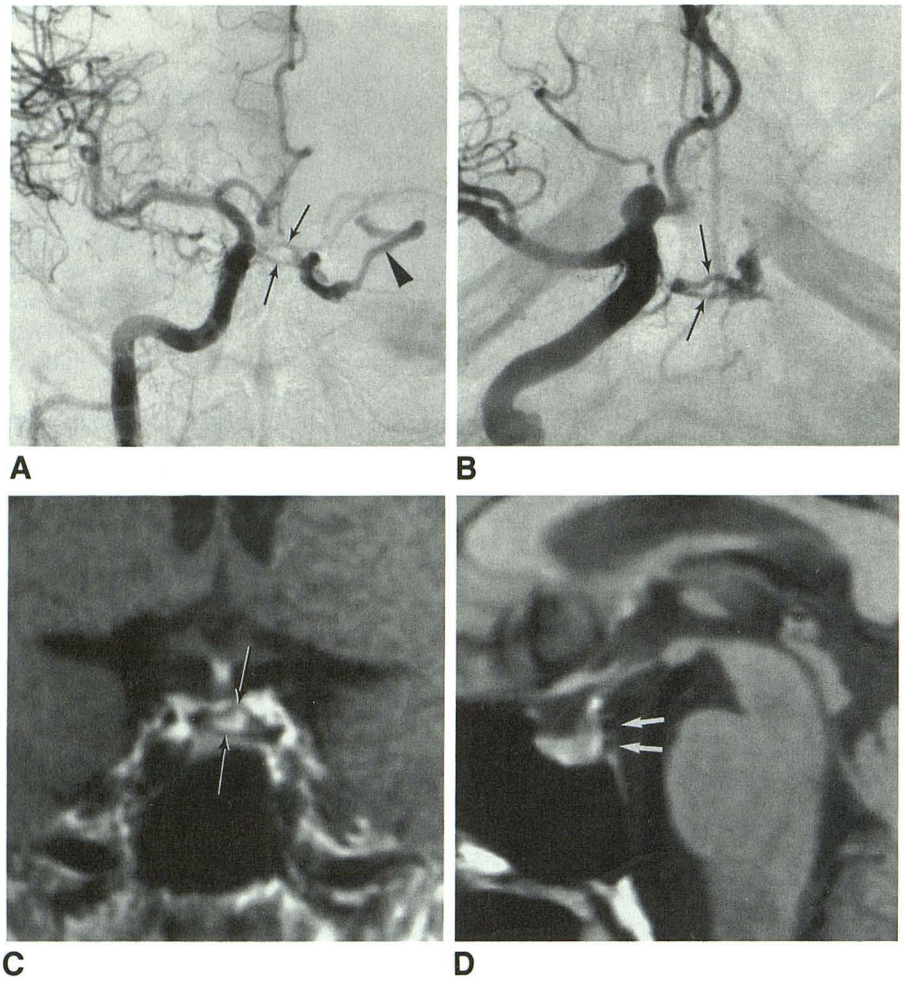

Fig. 3.—Case 3: 73-year-old woman with spontaneous carotid-dural vascular malformation.

***A*, Right carotid arteriogram, frontal view, shows right carotid-dural fistula with filling of two transsellar venous channels (*arrows*). Retrograde filling and distortion of contralateral superior ophthalmic vein is also seen (*arrowhead*).**

***B*, Base view demonstrates filling of two posteriorly placed venous channels (*arrows*).**

***C*, Coronal contrast-enhanced T1-weighted (600/20/2) MR image shows the two posteriorly located intercavernous sinuses (*arrows*).**

***D*, Sagittal T1-weighted (600/20/2) MR image shows that these vessels (*arrows*) probably lie within the dorsum sellae.**

Discussion

The anatomy and variations of the intercavernous sinuses have been documented in detail [1–4]. The basilar venous plexus is the largest intercavernous connection and has been consistently present in all studies [1–4]. It lies within dura posterior to the dorsum sellae and clivus and is plexiform in nature. This plexus interconnects not only the two cavernous sinuses but also the superior and inferior petrosal sinuses from side to side. The sixth cranial nerve passes through the basilar plexus to enter Dorello's canal beneath the petroclinoid ligament.

The anterior dural ICS (Figs. 1 and 4) is usually larger than the posterior or inferior sinuses, having been found in 27 of 27 injected specimens [1] and 38 of 50 dissected specimens [2]. The anterior ICS runs horizontally within dura posteroinferior to the tuberculum sellae. Its roof is formed by the anterior portion of the diaphragma sellae. An unusually large anterior sinus, found in five of 50 dissections [2], may extend into the dura anterior to the gland and is considered a disadvantage to transphenoidal surgery [2]. Once the anterior wall of the sella is removed during surgery, however, the periphery of the exposed dura is routinely cauterized prior to incision in order to prevent hemorrhage from this structure [5]. A cruciate incision is then made and the reflected dural leaves are again usually cauterized for hemostasis.

The posterior dural ICS (Fig. 4) has been found in 27 of 27 injected specimens [1] and 16 of 50 dissected specimens [2]. It runs horizontally within dura in front of the dorsum sellae but beneath the posterior clinoid processes. Its roof is formed by the posterior portion of the diaphragma sellae.

The inferior dural ICS (Figs. 2 and 5) has been found in eight of 27 injected specimens, usually as a complex of veins crossing the floor of the sella directly beneath the pituitary gland [1]. Another study [4] found a single transverse vein in this location in some cases but observed plexiform anatomy in others.

An additional intercavernous connection, known as the sinus of the dorsum sellae, has recently been described and likened to the basivertebral veins of the spine [6]. This sinus runs transversely within the bone of the dorsum sellae (Figs. 3 and 4) just inferior to the posterior clinoids and is typically 2 to 3 mm in diameter. Posteriorly, it is delimited by a thin shell of cortical bone or dura while anteriorly it is contained by cancellous bone. The sinus of the dorsum sellae has been found in 28 of 37 cadaver specimens [6]. It is apparently present to some degree in all specimens in which the dorsum sellae is not pneumatized.

Because of their small caliber, ICSs have received relatively little attention in the recent radiologic literature. Prior to the advent of high-resolution CT, venography of the cavernous sinuses and the ICS was performed to diagnose sellar and juxtasellar masses [4, 7, 8]. Bonneville et al. [9] have recently used dynamic contrast-enhanced CT in 680 patients with

Fig. 4.—Diagram illustrating the major parasellar venous connections. A = anterior intercavernous sinus, B = posterior intercavernous sinus, C = inferior intercavernous sinus, D = sinus of dorsum sellae, E = clival (basilar) plexus.

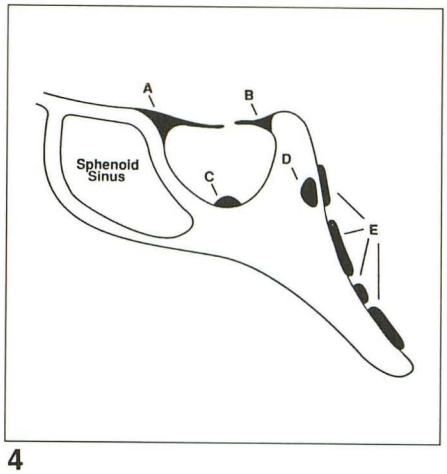

4

Fig. 5.—Sagittally cut cadaver specimen following venous injection with Latex illustrates some of the intercavernous sinus. *Large arrow* = anterior intercavernous sinus; *small arrow* = inferior intercavernous sinus, *curved arrow* = sinus of dorsum sellae, P = pituitary gland, S = sphenoid sinus.

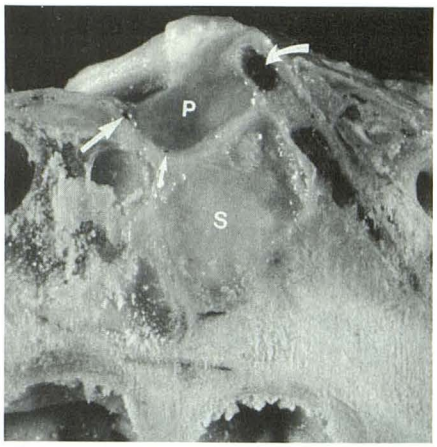

5

suspected pituitary lesions to demonstrate the basilar plexus as well as the anterior and inferior intercavernous connections. These investigators were unable to demonstrate the smaller posterior ICS, however.

Previous MR studies of the cavernous sinuses [10–13] have amply demonstrated the arteries, cranial nerves, and connective tissue structures within the cavernous sinuses, but have not discretely identified the ICS. In cases of CFs or dural arteriovenous malformations draining into the cavernous sinuses, the normal cavernous sinus signals on noncontrast MR have been reported to be distorted because of high-velocity time-of-flight signal losses and intravoxel phase dispersions [11–13]. These flow voids may represent either normal channels of rapidly flowing blood in the cavernous sinuses or actual venous structures contained within the cavernous sinuses. To our knowledge, dilatation of the ICS has not been previously recognized as a sign of either carotid-cavernous or carotid-dural fistulas on MR or CT.

With such a small series of patients, however, we must remain cautious about the absolute specificity of dilated ICS for the diagnosis of CFs. It is quite possible that dilated ICS will not be seen in all cases of CFs, such as those that drain wholly into the orbit or into the petrosal system. Distension of the ICS may not occur with very low-flow fistulas, although ICS engorgement was seen in the two patients in our series who had low-flow fistulas clinically. By similar reasoning it is entirely conceivable that a thrombus, mass, or inflammatory process in a cavernous sinus could cause shunting of blood with secondary dilatation of an ICS. Nevertheless, to our knowledge there have been no previous demonstrations of the ICS distending and filling at arteriography from any disease other than a CF or vascular malformation. We have looked for this sign retrospectively on the MR images of four patients with Tolosa-Hunt syndrome and one patient with cavernous sinus thrombosis, but have not seen it. Indeed, it seems doubtful whether simple shunting of venous blood around an obstructed cavernous sinus could produce the same dramatically dark flow voids in the ICS that we have demonstrated in cases of true CFs. Turbulent or rapid flow from an arterial source may be required to reduce the signal of the contrast-containing blood within the ICS to allow these vessels to be silhouetted against the adjacent enhancing pituitary gland or normal cavernous sinuses.

In many cases, the clinical diagnosis of CF is certain, requiring selective arteriography as the only diagnostic (and possibly therapeutic) procedure. In other cases, such as in two of the patients in this series, a relatively low-flow carotid-cavernous or carotid-dural fistula remains a reasonable diagnostic possibility, although other diseases need also be considered. In these situations, contrast-enhanced MR imaging may be the initial radiologic study. Recognition of dilated intercavernous vessels may potentially serve as a useful ancillary sign of CFs in these complicated cases.

REFERENCES

1. Winslow J. Cited by: Kaplan HA, Browder J, Krieger AJ. Intercavernous connections of the cavernous sinuses: the superior and inferior circular sinuses. *J Neurosurg* **1976**;45:166–168
2. Renn WH, Rhoton AL Jr. Microsurgical anatomy of the sellar region. *J Neurosurg* **1975**;43:288–298
3. Harris FS, Rhoton AL Jr. Anatomy of the cavernous sinus: a microsurgical study. *J Neurosurg* **1976**;45:169–180
4. Delvert JC, Théron J, Laffont J, Jan M, Santini JJ, Gouazé A. Anatomical bases of the radiological exploration of the intercavernous sinuses in the investigation of intrasellar expansive lesions. *Anat Clin* **1979**;1:301–307
5. Laws ER Jr. Transphenoidal approach to lesions in and about the sella turnica. In: Schmidek HH, Sweet WH, eds. *Operative neurosurgical techniques: indications, methods, and results*. Orlando: Grune and Stratton, **1988**:309–319
6. Schnitzlein HN, Murtagh FR, Arrington JA, Parkinson D. The sinus of the dorsum sellae. *Anat Rec* **1985**;213:587–589
7. Hanafee W, Rosen LM, Weidner W, Wilson GH. Venography of the cavernous sinus, orbital veins, and basal venous plexus. Work in progress. *Radiology* **1965**;84:751–753
8. Théron J, Chevalier D, Delvert M, Laffont J. Diagnosis of small and micro pituitary adenomas by intercavernous sinus venography. *Neuroradiology* **1979**;18:23–30
9. Bonneville JF, Cattin F, Racle A, et al. Dynamic CT of the laterosellar extradural venous spaces. *AJNR* **1989**;10:535–542
10. Daniels DL, Czervionke LF, Bonneville JF, et al. MR imaging of the cavernous sinus: value of spin echo and gradient recalled echo images. *AJNR* **1988**;9:947–952
11. Komiyama M, Yasui T, Baba M, Hakuba A, Nishimura S, Inoue Y. MR imaging of blood flows in the cavernous sinus. *Radiat Med* **1988**;6:124–129
12. Hirabuki N, Miura T, Mitomo M, et al. MR imaging of dural arteriovenous malformations with ocular signs. *Neuroradiology* **1988**;30:390–394
13. DeMarco JK, Dillon WP, Halbach VV, Tsuruda JS. Dural arteriovenous fistulas: evaluation with MR imaging. *Radiology* **1990**;175:193–199